

罗劬侃, 曹建华, 钟亮, 等. 铀同位素反演古海洋环境的研究进展[J]. 中国岩溶, 2024, 43(4): 957-968.

DOI: [10.11932/karst20240412](https://doi.org/10.11932/karst20240412)

## 铀同位素反演古海洋环境的研究进展

罗劬侃<sup>1,2,3</sup>, 曹建华<sup>2,3</sup>, 钟亮<sup>2,3</sup>, 白冰<sup>2,3</sup>, 王奇岗<sup>2,3,4</sup>, 廖红为<sup>2,3,5</sup>, 宗克清<sup>1</sup>, 覃汉莲<sup>2,3</sup>

(1. 中国地质大学地球科学学院, 湖北 武汉 430078; 2. 中国地质科学院岩溶地质研究所/自然资源部、广西岩溶动力学重点实验室/联合国教科文组织国际岩溶研究中心, 广西 桂林 541004; 3. 广西平果喀斯特生态系统国家野外科学观测研究站, 广西 平果 531406; 4. 中国地质大学环境学院, 湖北 武汉 430078;  
5. 中国地质大学地质探测与评估教育部重点实验室, 湖北 武汉 430078)

**摘要:** 铀同位素因可定量反演全球尺度古海洋缺氧洋底分布面积占比(%)而被广泛应用在埃迪卡拉纪末期以来的重要大洋缺氧或生物事件中。通过对国内外相关文献进行综述, 系统总结了利用铀同位素开展定量反演的原理、方法与成果, 初步构建了铀同位素定量反演的还原性海洋洋底面积占比(%)与大气氧气浓度、大洋缺氧或生物事件的耦合关系, 发现:(1)铀同位素反演结果与各缺氧或生物事件吻合度较高, 表明铀同位素确实为有效的全球尺度深时尺度定量反演指标;(2)还原性海洋洋底扩张与大气氧气浓度变化之间普遍存在滞后性, 推测与海平面、海洋生产力、海洋内部环流变化及底层水氧化还原反应的滞后性相关。指出铀同位素反演受样品后期成岩、风化蚀变作用的影响, 可能存在解译误差; 铀同位素单指标解译结果存在精准度偏低的缺点, 需采用多指标综合反演的方法提升反演精度。

**关键词:** 铀同位素; 定量反演; 铀同位素模型; 大洋缺氧; 生物事件

**创新点:** 构建了铀同位素定量反演的还原性洋底面积占比与大气氧气浓度、大洋缺氧或生物事件的耦合关系图; 发现还原性洋底扩张与大气氧气浓度变化并不一致, 推测与海平面、海洋生产力、海洋内部环流变化及底层水氧化还原反应滞后相关。

**中图分类号:** P736    **文献标识码:** A

**文章编号:** 1001-4810(2024)04-0957-12

**开放科学(资源服务)标识码(OSID):**



### 0 引言

显生宙以来, 全球经历多期次大洋缺氧事件<sup>[1-4]</sup>。海洋的氧化还原环境演变是对全球环境变化的重要响应, 有研究结果显示, 海洋氧化还原环境的演变可能与全球性大规模火山喷发<sup>[5-6]</sup>、海洋生产力提升<sup>[5-8]</sup>等息息相关, 常伴随海洋生物演替或大灭绝<sup>[9]</sup>, 尤其是中生代时期发生的大洋缺氧事件, 标志着白垩纪极端温室气候的开始、高潮与减弱<sup>[5]</sup>, 海洋的氧

化还原演变规律对探索现代气候变化并预测其发展趋势具有重要借鉴意义。

前人广泛使用地球化学示踪反演古海洋的氧化还原环境, 主要是采用对氧化还原环境敏感的元素(如 Cd、Ce、Co、Cr、Fe、Mo、Ni、S、Tl、V、U 等)开展相关研究<sup>[10-12]</sup>, 利用其在氧化和还原条件下不同的富集状态反映古海洋氧化还原环境。如 U、Mo、V、S 等在氧化状态下易迁移, 在还原状态下易沉淀; Fe 等在氧化条件下易沉淀, 在还原条件下易迁移; 在含

基金项目: 广西自然科学基金项目“<sup>238</sup>U/<sup>235</sup>U 对泥盆纪-石炭纪古海洋环境转型的指示意义——以桂林南边村全球辅助层型剖面为例”(2022GXNSFBA035593)

第一作者简介: 罗劬侃(1982—), 女, 副研究员, 硕士, 主要从事古环境重建方面的研究。E-mail: [luoqukan11@163.com](mailto:luoqukan11@163.com)。

收稿日期: 2023-06-25

硫的缺氧条件下, Fe、Cu、Zn 等元素易形成硫化物而沉淀<sup>[11-12]</sup>; Ni 在氧化状态形成可溶性化合物, 或以离子形式被腐殖酸或富里酸吸附, 在强还原状态下, Ni 可进入黄铁矿晶格被固定, 或与有机质络合进入沉积物<sup>[13-16]</sup>; V 则在氧化条件下易被铁锰氢氧化物或高岭石吸附, 在强还原条件下, 易被卟啉捕获, 或以氧化物或氢氧化物形式沉淀<sup>[17-18]</sup>。利用相关元素含量及 V/(V+Ni), U/Th, V/Cr 和 Ni/Co 比值可以作为古缺氧环境的判识标志<sup>[19-22]</sup>。但需要注意上述方法存在一定的局限性, 一是仅适用于对古海洋缺氧环境开展定性研究, 但无法定量反演各缺氧事件持续时间及扩张范围; 二是有机质的类型、沉积速率以及后期成岩作用等均可能影响相关结果的解译, 从而出现多解现象<sup>[23]</sup>。另外, 利用 I/Ca 比可半定量还原局部海洋的氧化还原条件, 即局部古海洋的溶氧量范围, 仍无法完全反映大洋缺氧事件持续的时间与范围<sup>[24]</sup>。除上述方法外, 前人广泛使用同位素方法来开展古海洋的氧化还原环境的定性研究, 目前最常用海相碳酸盐岩沉积物中的 C 同位素正负漂移对海洋氧化还原环境做定性研究, 其优点是可准确反映局部海洋氧化还原环境变化趋势, 缺点是无法反映全球范围内大洋缺氧事件发生范围及持续时间<sup>[23, 25-27]</sup>。利用 Mo 同位素可定量反映局部海洋氧化还原情况<sup>[28-29]</sup>, 但前提是只有在完全硫化的情况下, 沉积物中的 Mo 同位素组成才能代表当时古海洋的 Mo 同位素近似组成<sup>[23, 27-30]</sup>。利用 Tl 同位素, 也可定量还原全球尺度古海洋氧化还原环境, 但其受限于缺氧事件持续的时间尺度, 因其组成受控于 500 万年时间尺度内的锰的氧化物沉积, 而其在海洋中存在时间约为 18.5k 年, 故利用其同位素组成还原古海洋环境时, 对短时间尺度缺氧事件, 需要叠加分析锰的氧化物沉积带来的干扰<sup>[31]</sup>。

综上, U 同位素因其在全球海洋中的均一性, 且其组成与古海洋还原性洋底面积占比之间存在定量关系, 从而可定量反演不同时间段内全球尺度古海洋缺氧面积占比, 推导大洋缺氧事件持续时间尺度与扩张范围。近年来, U 同位素已被应用在埃迪卡拉纪末期、早寒武纪、奥陶纪/志留纪、晚泥盆纪弗拉期-法门期、泥盆纪/石炭纪、二叠纪/三叠纪、三叠纪/侏罗纪、二次大洋缺氧事件等关键大洋缺氧或生物事件中, 初步估算了不同时期大洋缺氧面积占比范围。U 同位素的定量反演结果为进一步探索古气

候变化趋势与诱因提供了更详实的数据支持, 有利于更加精准的构建古海洋氧化还原环境, 为预测未来海洋氧化还原演变趋势提供支撑。

## 1 原 理

### 1.1 铀的基本地球化学特性

铀在海洋中是一种保守元素, 铀在自然界中存在 3 种铀同位素:  $^{238}\text{U}$ 、 $^{235}\text{U}$ 、 $^{234}\text{U}$ , 天然铀是这 3 种同位素的混合物, 比例分别占 99.275%、0.72% 和 0.0054%, 这 3 种同位素均具有放射性, 半衰期分别为 4 468 Ma、703.8 Ma 和 0.248 Ma<sup>[32-33]</sup>。铀同位素在海水中可长期滞留, 滞留时间约为 0.32~0.56 Ma, 比海水充分混合的时间(约 1ka)长得多, 所以开放海中的 U 同位素组成是均匀的<sup>[34-35]</sup>; 因此, 从海水中沉积的碳酸盐岩有可能记录了全球海洋  $\delta^{238}\text{U}$ <sup>[36-39]</sup>。

铀具有+3、+4、+5 和+6 四种价态, 其中+4 和+6 价化合物相对稳定。在氧化状态下, 铀(+6 价)主要以可溶的碳酸铀酰基络合物离子存在于海洋中, 很容易融入海洋碳酸盐中, 无论生物成因或非生物成因, 同位素分馏相对有限<sup>[32, 35-36, 40-44]</sup>; 还原状态下, 铀(+4 价)相对不可溶并富集在海洋沉积物中。铀在还原过程中, 由于生物或非生物作用,  $^{238}\text{U}$  相对富集在沉积物中, 导致海水相对贫  $^{238}\text{U}$ 。

大量研究证实海相碳酸盐岩中的  $\delta^{238}\text{U}$  可以记录其沉积时原始海水中的  $\delta^{238}\text{U}$ <sup>[11, 13-14, 18-19]</sup>, 这些研究表明尽管原始碳酸盐沉积物展现出了变化范围极大的铀含量( $0.014 \times 10^{-6}$ ~ $3.6 \times 10^{-6}$ ), 但海洋各处的  $\delta^{238}\text{U}$  值大约为  $-0.40 \pm 0.15\text{‰}$ , 表明在碳酸钙从含水介质中沉积时, 仅发生了有限的铀同位素分馏。此外, 化石碳酸盐( $^{234}\text{U}/^{238}\text{U}$ )也证实海相碳酸盐沉积物保留了原始的  $\delta^{238}\text{U}$  特征<sup>[40-41]</sup>。

根据铀上述元素地球化学特征, 可利用海相碳酸盐沉积物中的铀同位素特征, 重建全球尺度的古海洋氧化还原环境<sup>[32, 35, 37, 45-50]</sup>。

### 1.2 海洋中铀同位素组成特征

在地表氧化环境中(如后太古代时期), 陆壳风化产生铀, 并通过河流转移, 可溶的 U(VI)流入海洋<sup>[36, 51]</sup>, 由于除了河流外的其他铀来源(如尘土、地下水等)非常微小, 且难以限定, 河流来源的铀被认为是海水铀的主要来源<sup>[34]</sup>, 大量研究表明河流

提供了海洋中 80%~100% 的铀<sup>[33, 52]</sup>, 一项综合性研究表明, 河流提供的铀大约为  $42 \times 10^6 \text{ mol/y}$ <sup>[34, 51]</sup>。全球河流铀通量指示的上地壳  $\delta^{238}\text{U}$  在误差范围内的值为  $0.29 \pm 0.03\text{\textperthousand}$ , 而现代海洋中  $\delta^{238}\text{U}$  为  $0.39 \pm 0.01\text{\textperthousand}$ <sup>[36, 41, 51, 53]</sup>。

铀从海水中剥离汇聚有几种汇, 包括还原性海洋(如局限洋盆)、还原性沉积物, 低温蚀变大洋洋壳, 这几种铀汇都富集铀的重同位素。还原性海洋是沉积物中铀汇的主要来源, 展示了最大的同位素分馏系数( $0.4\text{\textperthousand} \sim 1.2\text{\textperthousand}$ )<sup>[41, 54-56]</sup>, 使得还原性铀汇沉积成为全球海水铀同位素变化的主要原因。另一方面, 铀的轻同位素相对富集在金属沉积物(如铁锰结核)中(图 1)<sup>[36, 45, 57-59]</sup>。通常, 氧化-次氧化铀汇富集于单一的可移除汇。与还原态相比, 次氧化汇拥有可变的但相对小的分馏系数以及相对较低的铀沉积速率, 但在氧化海洋中, 次氧化铀汇代表的是单一的最大铀汇<sup>[50]</sup>。

### 1.3 利用铀反演古海洋氧化还原环境的原理

在现代海洋中, 还原性海洋洋底面积已经非常小了, 大约为 0.2%<sup>[60]</sup>, 与地球大部分历史时期一致, 海水中的  $\delta^{238}\text{U}$  是不变的, 大约为  $-0.4\text{\textperthousand}$ <sup>[32, 40-41]</sup>。如果碳酸盐岩未受成岩作用影响, 真实的记录了沉积时海水铀组成的话<sup>[32, 35, 40-41]</sup>, 那么碳酸盐岩  $\delta^{238}\text{U}$  应

该随着还原性洋底面积的扩张而降低。前文已经提到, 铀的存留时间( $3.2 \times 10^5 \sim 5.6 \times 10^5$  年)比海洋充分混合的时间要长( $10^3$  年), 那么局部区域的海洋铀组成(铀含量及  $\delta^{238}\text{U}$ )也即全球尺度的海洋铀组成。

铀含量及  $\delta^{238}\text{U}$  对洋底氧化还原环境范围变化的独特敏感性可分别通过海水铀含量及其同位素组成的微分质量守恒方程(如 Lau 方程与 Gilleadeau 方程)表示。通过质量守恒方程的变换式, 可计算出还原性海洋洋底面积占比, 从而定量反演出某一时段古海洋的还原化程度。前文已提及海相碳酸盐岩沉积物中的铀同位素组成可以代表当时古海洋铀同位素组成, 通过测试不同年代海相碳酸盐岩沉积物中的  $\delta^{238}\text{U}$ , 可推测不同年代古海洋的缺氧程度, 从而可对古海洋缺氧程度与持续时间进行系统重建。

## 2 方法

根据质量守恒方程, Lau 等于 2016 年提出了首个铀汇箱式模型<sup>[37]</sup>, 利用  $\delta^{238}\text{U}$  及铀含量来计算古海洋还原性洋底面积占比, 后来的研究人员在此基础上不断变换方程, 形成了以该方程为基础的系列变体, 用于简化相关计算; 至 2019 年, Gilleadeau 等根

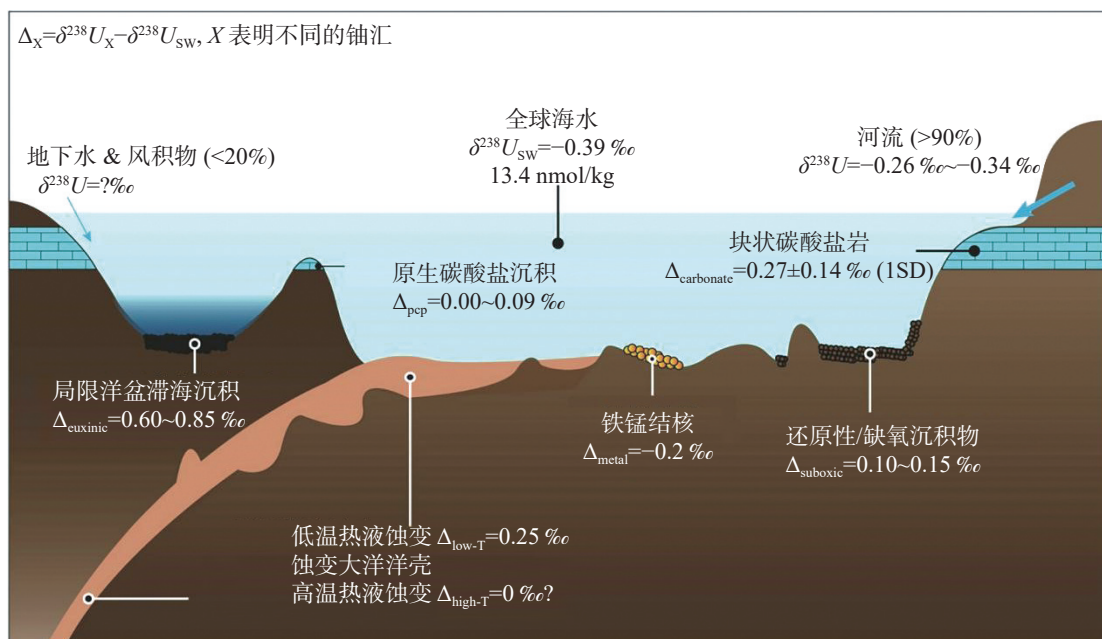


图 1 海洋中铀同位素平衡模型(海洋中主要的溶解铀来源于陆地河流, 海洋铀会包括还原性/缺氧沉积物、局限性滞海洋盆沉积、海相碳酸盐、铁锰结核及蚀变大洋洋壳)(据 [59])

Fig. 1 U isotope budget model in the oceans (The main sources of dissolved uranium in the ocean are terrestrial rivers, and marine uranium can include reduced/anoxic sediments, localized stagnant ocean basin deposits, marine carbonates, ferromanganese-manganese nodules, and altered macrocrust) (According to [59])

据不同铀汇的主次关系,提出了三类铀汇箱式模型<sup>[49]</sup>,属于 Lau 方程变体中较为独特的一种应用手段。

## 2.1 铀汇箱式模型 (LAU 方程)

$\delta^{238}\text{U}$  和铀含量对还原性洋底面积变化的敏感性可分别由下列质量守恒方程表示:

$$\frac{dN_{sw}}{dt} = J_{riv} - J_{anox} - J_{other} \quad (1)$$

$$\frac{N_{sw} \times d\delta^{238} U_{sw}}{dt} = J_{riv} \times (\delta^{238} U_{riv} - \delta^{238} U_{sw}) - J_{anox} \times \Delta_{anox} - J_{other} \times \Delta_{other} \quad (2)$$

其中,  $N_{sw}$  是指海洋中铀的总含量摩尔数,  $\delta^{238}\text{U}$  是海水中的 $\delta^{238}\text{U}$  分馏系数,  $\delta^{238} U_{riv}$  是河源 $\delta^{238}\text{U}$  分馏系数,  $\Delta_{anox} = +0.6\text{\textperthousand}$  是还原性铀汇的有效分馏系数<sup>[41]</sup>,  $\Delta_{other}$  是其他铀汇的有效分馏系数(计 $+0.03\text{\textperthousand}$ , 根据现代海洋稳定态化学特征计算<sup>[45,61]</sup>), 式中将铀的输入通量简化为河源铀  $J_{riv}$ [ 现代海洋数据为  $0.4 \times 10^8 \text{ mol U/y}$ <sup>[52]</sup>], 输出通量则被认为是由还原性铀汇( $J_{anox}$ )和其他铀汇( $J_{other}$ )组成。这里还原性铀汇通量为  $J_{anox} = 0.06 \times 10^8 \text{ mol U/y}$ <sup>[52]</sup>, 而根据初始稳定状态获取的质量守恒方程得  $J_{other} = 0.34 \times 10^8 \text{ mol U/y}$ , 进一步定义输出通量为:

$$J_{anox} = K_{anox} \times N_{sw} \times f_{anox} \quad (3)$$

$$J_{other} = K_{other} \times N_{sw} \times (1 - f_{anox}) \quad (4)$$

这里,  $f_{anox}$  是还原性洋底面积占比,  $K_{anox}$  和  $K_{other}$  是现代铀系的转换常数, 假设在整个研究期, 沉积物—水界面(SWI)铀还原机制一致,  $K_{anox}$  认为是恒定的, 同理,  $K_{other}$  也被认为是恒定的。估算碳酸盐中的铀含量可认为是海水中铀含量的转移, 并假设海水钙的集中与分布系数恒定为 1.4<sup>[62]</sup>。

假设整个地质历史时期各相关元素地球化学行为恒定, 可得到下列转换后的方程以计算还原性洋底面积占比  $f_{anox}$ , 从而可得知不同历史时期还原性海洋面积占比变化趋势, 并判断各时期海洋的氧化还原环境。

$$N_{sw} = \frac{J_{riv}}{K_{anox} \times f_{anox} + K_{other} \times (1 - f_{anox})} \quad (5)$$

$$\delta^{238} U_{sw} = \delta^{238} U_{riv} - \frac{N_{sw} \times [K_{other} \times \Delta_{other} + f_{anox} \times (K_{anox} \times \Delta_{anox} - K_{other} \times \Delta_{other})]}{J_{riv}} \quad (6)$$

Lau 认为海洋中主要有 5 种铀汇, 即 1)还原环境(包括含 S 和不含 S)产生的铀汇为 $\sim 7\text{--}12 \text{ Mmol/y}$ ,

占总 U 汇的 15%~24%<sup>[34,36]</sup>, 与现代海洋相比, 其  $\delta^{238}\text{U}$  比海洋正偏 0.35‰~0.80‰<sup>[63\text{--}66]</sup>; 2)次氧化环境产生的铀汇, 尽管比还原环境产生的 U 汇小一个数量级, 但其分布广泛, 其  $\delta^{238}\text{U}$  与海洋相比轻微正偏<sup>[32,34,41]</sup>; 3) Fe、Mn 氧化物吸收产生的铀汇为 $\sim 1.6\text{--}6 \text{ Mmol/y}$ , 占总铀汇的 2%<sup>[34,52]</sup>, 与现代海洋相比, 其  $\delta^{238}\text{U}$  比海洋负偏 $\sim 0.24\text{\textperthousand}$ <sup>[32,45,57]</sup>; 4)玄武岩热液蚀变产生的铀汇为 $5.7\text{--}27 \text{ Mmol/y}$ , 占总铀汇的 12%, 但其分馏系数较小, 约为 0.2‰<sup>[67]</sup>; 5)生物碳酸盐和硅质岩产生的铀汇, 约占总铀汇的 30%, 但其分馏系数最小<sup>[34]</sup>。

总体而言, 碳酸盐铀含量及同位素组成对河源输入通量、同位素组成、铀在碳酸钙中(在 LAU 方程中取平均值为 1.4)的分布系数( $D_U$ )紧密相关, 改变其中任何一个参数, 仅能改变铀含量或  $\delta^{238}\text{U}$  中的一个参数, 但无法同时改变其数值。只有改变了初始的  $f_{anox}$  数值, 才可能同时改变铀含量和  $\delta^{238}\text{U}$ , 该箱式模型可以预测出还原性洋底的最大面积范围, 改变大部分变量(如  $J_{riv}$ 、 $\delta^{238} U_{riv}$ 、 $D_U$ )仅能改变预测曲线的绝对值, 但曲线变化趋势未变, 只有在改变有效分馏系数  $\Delta_{anox}$  和  $f_{anox}$  会改变  $\delta^{238}\text{U}$  的偏移数量级, 以及铀含量和  $\delta^{238}\text{U}$  的变化速率(图 2)。

Lau 方程为后续利用铀的同位素组成特征对海洋氧化还原环境进行定量研究提供了关键基础, 后来的研究人员常用的定量研究方程均为 Lau 方程的变换式, 并在计算其他铀汇时, 往往将铁锰氧化物吸收产生的铀汇、玄武岩热液蚀变产生的铀汇以及生物碳酸盐和硅质岩产生的铀汇忽略不计。

## 2.2 三类铀汇质量守恒模型 (Gilleadeau 方程)

与 Lau 方程不同, Gilleadeau 将 Lau 方程简化, 在其定量估算中元古代海洋还原性海洋洋底面积占比时, 采用了三类铀汇质量守恒模型, 即: (1)含 S 的还原性沉积物形成的铀汇, 与海水铀同位素组成相比, 偏移了 0.4‰~1.2‰(铀汇—海水); (2)还原性沉积物(不含 S)形成的铀汇, 与海水相比, 偏移了 0.2‰~0.4‰; (3)氧化性沉积物形成的铀汇, 与海水相比, 偏移了 $-0.2\text{\textperthousand}$ <sup>[11,14,31\text{--}32,35]</sup>。在上述参数基础上, Gilleadeau 建立了三类铀汇质量守恒模型:

$$\delta^{238} U_{sw} = \delta^{238} U_{input} - \frac{(k_{eux} A_{eux} \Delta_{eux} + k_{anox} A_{anox} \Delta_{anox} + k_{ox} A_{ox} \Delta_{ox})}{k_{eux} A_{eux} + k_{anox} A_{anox} + k_{ox} A_{ox}} \quad (7)$$

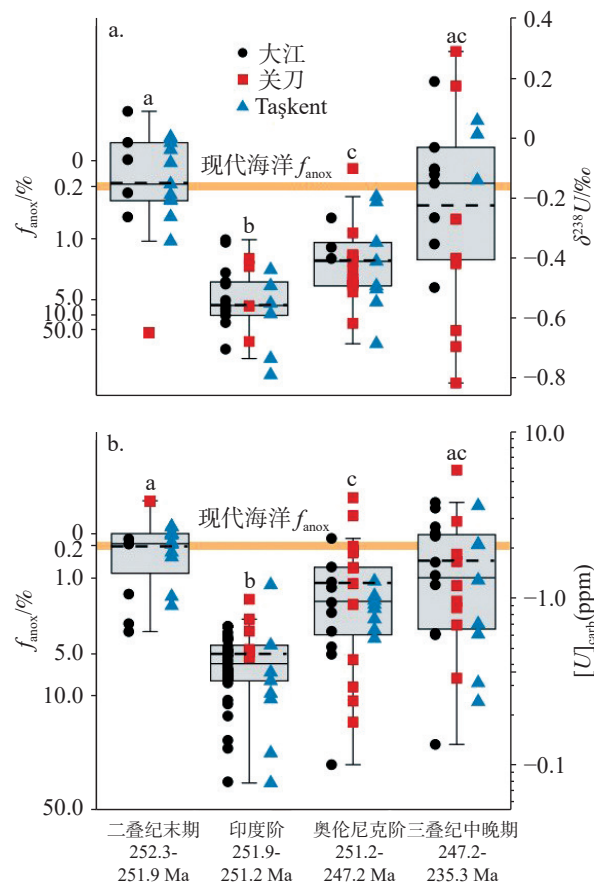


图2 利用Lau铀汇箱式模型(A图: $\delta^{238}\text{U}$ 和B图:[U]值)计算出晚二叠纪-中晚三叠纪古海洋还原性面积占比 $f_{\text{anox}}$ (据文献[37])

注:虚线为平均值,延长线上、下端为最大和最小值

Fig. 2 Proportion of anoxic seafloor area ( $f_{\text{anox}}$ , %) of Late Permian–Late-Middle Triassic by using Uranium Box Model  
(Figure A:  $\delta^{238}\text{U}$  and Figure B: [U] value)  
(According to literature[37])

Note: The dotted line is the average value, and the upper and lower ends of the extension line are the maximum and minimum values.

式中的 $\delta^{238}\text{U}_{\text{input}}$ 表明河源铀组成特征, $\Delta$ 表示不同铀汇相对海水铀组成的有效分馏系数( $\delta^{238}\text{U}_{\text{sink}}-\delta^{238}\text{U}_{\text{sw}}$ ), $A$ 表示各类海洋洋底面积占比, $k$ 表示铀形成铀汇的一级常数。

通过上述方程变换,我们可以在 $\delta^{238}\text{U}_{\text{sw}}$ 给定的情况下,计算出不同组合的洋底面积占比( $A_{\text{ox}}$ ,  $A_{\text{anox}}$ 和 $A_{\text{eux}}$ )。我们通过以下方程,可以计算出模型中氧化性海洋最大面积占比( $A_{\text{ox}}$ ),即假设海洋中的铀汇仅为含S的还原性沉积物(封闭海)形成的铀汇和氧化性沉积物形成的铀汇:

$$A_{\text{ox}} = \frac{(\delta^{238}\text{U}_{\text{input}} - \delta^{238}\text{U}_{\text{sw}})k_{\text{eux}} - k_{\text{eux}}\Delta_{\text{eux}}}{k_{\text{ox}}\Delta_{\text{ox}} - k_{\text{eux}}\Delta_{\text{eux}} - (\delta^{238}\text{U}_{\text{input}} - \delta^{238}\text{U}_{\text{sw}})(k_{\text{ox}} - k_{\text{anox}})} \quad (8)$$

以及通过以下方程,可以计算出模型中氧化性

海洋最小面积占比( $A_{\text{anox}}$ ),即假设海洋中的铀汇仅为不含S的还原性沉积物形成的铀汇和氧化性沉积物形成的铀汇:

$$A_{\text{anox}} = \frac{(\delta^{238}\text{U}_{\text{input}} - \delta^{238}\text{U}_{\text{sw}})k_{\text{anox}} - k_{\text{anox}}\Delta_{\text{anox}}}{k_{\text{ox}}\Delta_{\text{ox}} - k_{\text{anox}}\Delta_{\text{anox}} - (\delta^{238}\text{U}_{\text{input}} - \delta^{238}\text{U}_{\text{sw}})(k_{\text{ox}} - k_{\text{anox}})} \quad (9)$$

通过相同的方法可计算出最大和最小 $A_{\text{anox}}$ 和 $A_{\text{eux}}$ 。

总体而言,Gilleaudeau方程是将Lau方程中所提到的五种铀汇的简化方程,在Gilleaudeau运用该简化方程计算中元古代含硫的还原性海洋(静海或封闭海)洋底面积占比时,可得到唯一解,且与其他研究手段得出的结果相一致;但在估算中元古代不含硫的还原性海洋和氧化性海洋洋底面积占比时却无法得到唯一解(图3),还需要辅以其他研究手段,如微量金属元素、钼同位素等。

### 3 成果

#### 3.1 埃迪卡拉纪以来还原性洋底面积(%)与重要大洋缺氧及生物事件耦合关系

通过铀同位素平衡方程可以推定地质历史时期还原性洋底面积占比,结合Reershemius等<sup>[68]</sup>总结的显生宙以来大洋缺氧事件与大气氧气浓度变化图,可初步构建大洋还原性洋底面积占比、大气氧气浓度、大洋缺氧事件及生物事件的耦合关系图,从而直观的反映古气候的变化特征及其对生物演化产生的影响。本文选取了埃迪卡拉纪以来发生的八大典型生物事件及大洋缺氧事件,即埃迪卡拉纪末期、早寒武纪、奥陶纪/志留纪、晚泥盆纪弗拉期—法门期、泥盆纪/石炭纪、二叠纪/三叠纪、侏罗纪和二次大洋缺氧事件。

(1) 埃迪卡拉纪末期(~550—541Ma): Zhang等<sup>[56]</sup>、Tostevin等<sup>[69]</sup>计算出埃迪卡拉纪末期还原性海洋洋底最小面积占比约为21%~33%,属于还原性海洋洋底扩张时期,并认为其扩张可能降低了生物群落多样性乃至动物活性等,从而引起这一时期的生物大灭绝;同一时期,大气氧气浓度<5%,且持续下降<sup>[69]</sup>,此时大气氧气浓度变化趋势与缺氧海底扩张趋势相吻合。

(2) 早寒武纪(~538—520Ma): Wei等<sup>[70-71]</sup>以及Dahl等<sup>[72]</sup>计算出早寒武纪还原性洋底面积占比在

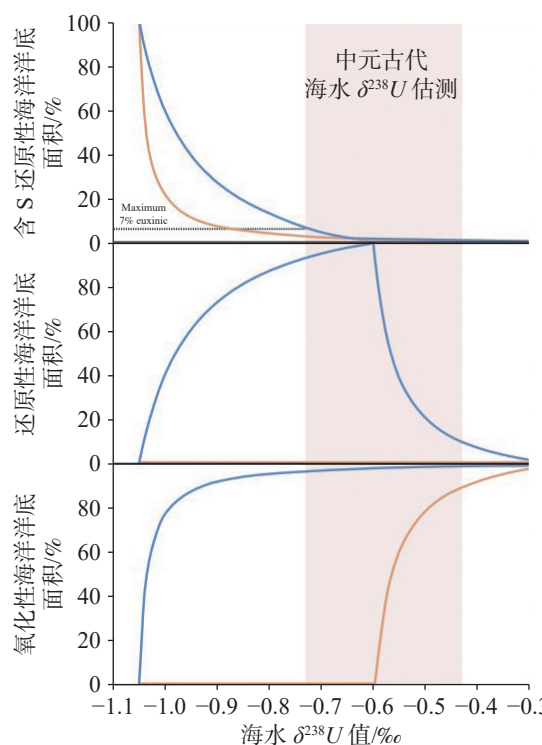


图 3 中元古代海洋三类铀汇质量守恒模型测算  
(据文献 [49])

橙线代表各种可能的模型迭代下的最小洋底面积, 蓝色代表最大洋底面积, 红色块状部分为中元古代海水  $\delta^{238}\text{U}_{\text{sw}}$  ( $-0.43\%$  至  $-0.73\%$ ) $\text{‰}$ , 图中虚线交汇处, 代表含 S 的还原性静海洋底面积占比最大为 7%。

Fig. 3 Estimation of three-sink mass balance modeling on Mid-Proterozoic seawater (According to literature [49])

The orange line represents the minimum seafloor area under various possible model iterations; the blue line represents the maximum seafloor area, and the red block represents the  $\delta^{238}\text{U}_{\text{sw}}$  ( $-0.43\%$  to  $-0.73\%$ ) $\text{‰}$  of the Mesoproterozoic seawater. The intersection of dotted lines in the figure represents the maximum 7% of the seafloor area of the anoxic quiet sea containing S.

$<\sim 10\%$  到  $>\sim 50\%$  之间变化, 在峰值区域可达  $70\% \sim 80\%$ , 此时大气氧气浓度在  $\sim 2.5\% \sim 10\%$  变化, 且起伏较大, 对应还原性海洋洋底面积急剧变化, 表明地球这一时期处于氧化和还原的急剧交替状态, Wei 等人认为波动的海洋缺氧状态更有利于促进生物演替和生态结构重构, 是寒武纪生命大爆发的主要推动因素<sup>[70]</sup>。

(3) 奥陶纪/志留纪 ( $\sim 445.2$ — $443.8\text{ Ma}$ ): Bartlett 等人计算出赫南特期(HOAE)还原性海洋洋底面积占比大约增加了 15%, 为  $\sim 9\% \sim 13.5\%$ <sup>[71]</sup>, 认为其原因是全球变冷影响了热盐环流, 降低了深海通风效率, 增加了营养元素通量, 刺激了生产力, 使得“最小含氧带”(OMZ)得以扩张<sup>[72]</sup>, 恰与奥陶纪末期生物大灭绝事件相吻合。同一时期, 大气氧气浓度却处于从

奥陶纪中晚期谷底值开始逐渐上升的阶段。

(4) 晚泥盆纪弗拉期—法门期 ( $\sim 376$ — $370\text{ Ma}$ ): White 等计算出晚泥盆纪弗拉期-法门期还原性海洋洋底面积占比增长了  $\sim 5\% \sim 15\%$ , 为  $\sim 44\% \sim 55\%$ , 模型估测峰值为  $\sim 70\%$ <sup>[74]</sup>, 表明海洋缺氧洋底在这一时期经历了快速扩张时期, 恰好与同一时段生物大灭绝事件吻合; 同一时期, 大气氧气浓度却处于从泥盆纪中晚期谷底值逐步上升的阶段。

(5) 泥盆纪/石炭纪 ( $\sim 359.9$ — $358.9\text{ Ma}$ ): Zhang 等人估测出泥盆纪末期还原性海洋洋底面积占比为  $\sim 5\% \sim 15\%$ , 还原性海洋的快速扩张与 Hangenberg 事件开始发生的时间相吻合, 表明大洋缺氧确实是导致该灭绝事件发生的重要因素之一, 并认为泥盆纪末期种子植物的扩张带来的深部根系发育增强了大陆风化, 并引起了还原性海洋的快速扩张和其他地球变化<sup>[59]</sup>; 同一时期, 大气氧气浓度也处于从泥盆纪晚期谷底值逐步上升的阶段。

(6) 二叠纪/三叠纪 ( $\sim 252.4$ — $251.4\text{ Ma}$ ): Zhang 等<sup>[75]</sup>、Lau 等<sup>[37]</sup>、Elrick 等<sup>[48]</sup>估测出这一时段还原性洋底面积占比为  $\sim 5\% \sim 20\%$ , Zhang 等<sup>[75]</sup>认为火山喷发以及磷风化速率的增加恰好与大洋缺氧事件吻合, 证明二叠纪末期大洋缺氧事件确实经历了快速动荡时期, 也与这一时期发生的生物大灭绝事件相吻合; 同一时期, 大气氧气浓度处于二叠纪末期短时间尺度内的相对峰值状态。

(7) 三叠纪/侏罗纪 ( $\sim 201.5$ — $200\text{ Ma}$ ): Jost 等<sup>[76]</sup>研究认为这一时期, 还原性海洋洋底面积占比先达到  $8\% \sim 20\%$ , 持续大约 4.4 万年, 而后降低至  $0.6\% \sim 6\%$ , 并持续约 20 万年, 也较好地吻合了同一时期发生的生物大灭绝事件; 这一时期大气氧气浓度则处于从三叠纪中晚期的相对峰值逐步下降的时期。

(8) 二次大洋缺氧事件 ( $\sim 94\text{ Ma}$ ): Clarkson 等<sup>[8]</sup>根据模型计算出这一时期还原性海洋洋底面积占比约为  $8\% \sim 15\%$ , 并认为是大火成岩省引起大气  $\text{CO}_2$  的快速增加而导致的; 同一时期, 大气氧气浓度处于相对低谷时期。

### 3.2 讨论

为方便讨论, 图 4 中主要展示了还原性洋底面积的峰值变化范围, 由于 Krause 模型<sup>[77]</sup>估测出的大气氧气浓度更贴合不同研究手段反映出的大气氧气

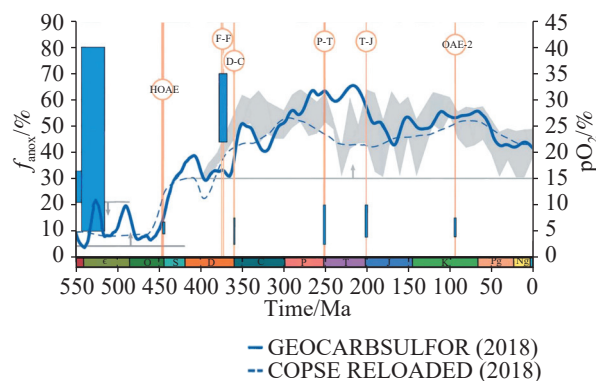


图4 显生宙主要大洋缺氧事件(或生物大灭绝/生命大爆发事件)发生时期大气氧气浓度与还原性洋底面积占比变化耦合关系图(据[68]修改)

注:深蓝色实线为GEOCARBSULFOR生物地球化学模型模拟出的大气氧气含量变化范围<sup>[77]</sup>;深蓝色虚线为COPSE生物地球化学模型模拟出的大气氧气含量变化范围<sup>[78]</sup>;灰色不规则区域代表通过化石木炭重建的大气氧气含量变化曲线<sup>[79]</sup>。灰色线条代表通过地球化学指标、寒武纪生物群和大火燃烧记录重建的大气氧气浓度阈值<sup>[80-84]</sup>。浅蓝色方框代表对应年代还原性海洋洋底面积占比变化范围。

Fig. 4 Coupling relationship between atmospheric oxygenation concentration, anoxic seafloor area ( $f_{\text{anox}}$ , %) during the oceanic anoxic events (or mass extinction/life explosion)

(Modified based on [68])

Note: The deep blue solid line represents the range of atmospheric oxygen content simulated by the GEOCARBSULFOR biogeochemical model<sup>[77]</sup>; the deep blue dashed line represents the range of atmospheric oxygen content simulated by the COPSE biogeochemical model<sup>[78]</sup>; the gray irregular region represents the curve of atmospheric oxygen content change reconstructed from fossil charcoal<sup>[79]</sup>. The gray lines represent the threshold values of atmospheric oxygen concentration reconstructed from geochemical indicators, Cambrian biota, and fire burning records<sup>[80-84]</sup>. The light blue box represents the range of the proportion of anoxic seafloor area for the corresponding period.

浓度实际变化情况,下文论述时,大气氧气浓度均采用Krause的模型估测结果。

首先,从上述耦合关系图中可以发现U同位素定量反演结果较好地贴合了大洋缺氧事件和生物事件,尤其是较好印证了埃迪卡拉纪末期、奥陶纪末期、晚泥盆纪弗拉期-法门期、泥盆纪/石炭纪、二叠纪/三叠纪、三叠纪/侏罗纪发生的生物大灭绝事件,同时海洋氧化与还原状态的急剧波动,又较好印证了早寒武纪时期发生的生命大爆发。由此可以得出铀同位素是定量反演全球尺度深时古海洋氧化还原环境演变的有效指标。

其次,从上述耦合关系图中可以发现,海洋还原性洋底面积的扩张与大气O<sub>2</sub>浓度变化并不完全同步,如赫南特期、弗拉期-法门期、泥盆纪/石炭纪、二

叠纪/三叠纪、三叠纪/侏罗纪发生还原性海洋洋底扩张事件时,大气氧气浓度并未处于相对谷底值,通常处于上一谷底值的上升阶段,仅三叠纪/侏罗纪的大气氧气浓度处于上一峰值的下降阶段。这说明,还原性海洋洋底的扩张往往滞后于大气氧气浓度的变化。分析认为铀同位素反演结果指示的是缺氧洋底面积占比,即还原性海水水柱的底面积占比,实际是海洋底层水的氧化还原状态的变化;大气氧气浓度变化,首先影响浅层海水,其优先响应大气氧化还原环境的变化,而后逐步影响水体中的生物生产力,逐渐将氧化还原演化导致的环境变化传导至底层水,并因此导致还原性海洋洋底扩张或收缩的滞后反应;或因气温变化,导致海平面升降等,引起海洋内部环流(如热盐环流)变化从而引起生产力变化,并导致海水内部发生还原性洋底面积扩张或收缩,同样产生了滞后效应。大气氧化还原演化与海洋洋底氧化还原演化之间的耦合关系应是未来探索研究的重点,可通过探索自然或人类影响下海洋氧化还原演化的时间效应来预测未来海洋环境演化趋势。

## 4 展望

综上,铀同位素因其独特的地球化学特性,可用来定量研究全球尺度古海洋的缺氧范围以及持续时间,是对古气候环境变化的重要定量化研究手段。但是,在现有技术方法的应用过程中,仍然发现该方法存在有待完善的地方,未来需要在以下领域进一步完善:

(1)首先,铀同位素虽已在埃迪卡拉纪以来的大部分重要生物事件和大洋缺氧事件中得以运用,但是部分研究成果的取样地代表性还有待完善,虽然理论上铀同位素具有全球均一性,但这一论断没有充分考虑各取样地后期成岩、风化蚀变作用等对原始海水中铀同位素组成的影响,有必要针对同一事件采用不同取样地样品进行校准验证,以进一步提高定量研究精度。

(2)铀同位素单指标反演结果存在反演范围过广,结果精度不足的情况。有必要开展多指标同位素综合定量反演,比如Mo、Tl等,也可有效提高同一事件的反演精度。

(3)在进一步改善铀同位素反演精度的基础上,可以利用铀同位素等综合定量反演方法推导大气氧

化还原演化与海洋氧化还原演化之间的耦合关系(尤其是海洋氧化还原演化的时间效应),从而可以从现代大气环境演化(自然和人为因素)推导出某一段时间段后海洋发生氧化还原演化的影响范围与影响程度,为人类应对全球变化提供支撑。

## 参考文献

- [1] Kaiho K, Kajiwara Y, Tazaki K, et al. Oceanic primary productivity and dissolved oxygen levels at the Cretaceous/Tertiary boundary: Their decrease, subsequent warming, and recovery[J]. *Palaeoceanography*, 1999, 14(4): 511-524.
- [2] Isozaki Y. Permian-Triassic boundary superanoxia and stratified superocean: Records from lost deep sea[J]. *Science*, 1997, 276: 235-238.
- [3] Bratton J F, Berry W B N, Morrow J R. Anoxia predates Frasnian-Famennian boundary mass extinction horizon in the Great Basin, USA[J]. *Palaeogeography, Palaeoclimatology, Palaeoecology*, 1999, 154: 275-292.
- [4] Turgeon S C, Brumsack H J. Anoxic vs dysoxic events reflected in sediment geochemistry during the Cenomanian-Turonian Boundary Event (Cretaceous) in the Umbria-Marche Basin of Central Italy[J]. *Chemical Geology*, 2006, 234: 321-339.
- [5] 黄永建,王成善,顾健.白垩纪大洋缺氧事件:研究进展与未来展望[J].*地质学报*,2008,82(1):21-30.
- HUANG Yongjian, WANG Chengshan, GU Jian. Cretaceous Oceanic Anoxic Events: Research progress and forthcoming prospects[J]. *Acta Geologica Sinica*, 2008, 82(1): 21-30.
- [6] 陈曦,郭会芳,姚翰威,韩凯博,汪恒慧.白垩纪大洋缺氧事件OAE2期间碳循环扰动的过程与机制[J].科学通报,2022,67(15): 1677-1688.
- CHEN Xi, GUO Huifang, YAO Hanwei, HAN Kaibo, WANG Henghui. Processes and forcing mechanisms of the carbon cycle perturbation during Cretaceous Oceanic Anoxic Event 2[J]. *Chinese Science Bulletin*, 2022, 67(15): 1677-1688.
- [7] 常华进,储雪蕾,冯连君,黄晶,张启锐.氧化还原敏感微量元素对古海洋沉积环境的指示意义[J].*地质论评*,2009,55(1): 91-99.
- CHANG Huajin, CHU Xuelei, FENG Lianjun, HUANG Jing, ZHANG Qirui. Redox sensitive trace elements as paleoenvironments proxies[J]. *Geological Review*, 2009, 55(1): 91-99.
- [8] Clarkson M O, Stirling C H, Jenkyns H C, et al. Uranium isotope evidence for two episodes of deoxygenation during Oceanic Anoxic Event 2[J]. *Proceedings of the National Academy of Sciences of the United States of America*, 2018, 115(12): 2918-2923.
- [9] Jenkyns H C. Geochemistry of Oceanic Anoxic Events[J]. *Geochemistry Geophysics Geosystems*, 2010, 11(3): Q03004.
- [10] Francois R. A study on the regulation of the concentrations of some trace metals (Rb, Sr, Zn, Pb, Cu, V, Cr, Ni, Mn and Mo) in Saanich Inlet Sediments, British Columbia, Canada[J]. *Marine Geology*, 1988, 83(1/2/3/4): 285-308.
- [11] Russell A D, Morford J L. The behavior of redox-sensitive metals across a laminated-massive-laminated transition in Saanich Inlet, British Columbia[J]. *Marine Geology*, 2001, 174(1/2/3/4): 341-354.
- [12] Algeo T J. Can marine anoxic events draw down the trace element inventory of seawater?[J]. *Geology*, 2004, 32: 1057-1060.
- [13] Calvert S E, Pedersen T F. Geochemistry of recent oxic and anoxic marine sediments: Implications for the geological record[J]. *Marine Geology*, 1993, 113(1/2): 67-88.
- [14] Piper D Z, Perkins R B. A modern vs. Permian black shale: The hydrography, primary productivity, and water-column chemistry of deposition[J]. *Chemical Geology*, 2004, 206(3/4): 177-197.
- [15] Morse J W, Luther G W III. Chemical influences on trace metal-sulfide interactions in anoxic sediments[J]. *Geochimica et Cosmochimica Acta*, 1999, 63(19/20): 3373-3378.
- [16] Grosjean E, Adam P, Connan J, Albrecht P. Effects of weathering on nickel and vanadyl porphyrins of a Lower Toarcian shale of the Paris basin[J]. *Geochimica et Cosmochimica Acta*, 2004, 68(4): 789-804.
- [17] Wanty R B, Goldhaber M B. Thermodynamics and kinetics of reactions involving vanadium in natural systems: Accumulation of vanadium in sedimentary rocks[J]. *Geochimica et Cosmochimica Acta*, 1992, 56 (4): 1471-1483.
- [18] Morford J L, Emerson S. The geochemistry of redox sensitive trace metals in sediments[J]. *Geochimica et Cosmochimica Acta*, 1999, 63 (11/12): 1735-1750.
- [19] Tyson R V, Pearson T H. Modern and ancient continental shelf anoxia: An overview[J]. *Geological Society, London, Spec Publications*, 1991, 58: 1-24.
- [20] Hatch J R, Leventhal J S. Relationship between inferred redox potential of the depositional environment and geochemistry of the Upper Pennsylvanian (Missourian) Stark Shale Member of the Dennis Limestone, Wabaunsee County, Kansas, U. S. A.[J]. *Chemical Geology*, 1992, 99: 65-82.
- [21] Bryn Jones, David A C Manning. Comparison of geochemical indices used for the interpretation of palaeoredox conditions in ancient mudstones[J]. *Chemical Geology*, 1994, 111: 111-129.
- [22] Wignall P B. Black Shale[M]. Oxford: Clarendon Press, 1994.
- [23] 周炼,苏洁,黄俊华,颜佳新,解习农,高山,戴梦宁,腾格尔.判识缺氧事件的地球化学新标志—钼同位素[J].*中国科学:地球科学*,2011,41(3): 309-319.
- [24] 尚墨翰,汤冬杰,史晓颖,魏昊明,刘安琪. I/(Ca+Mg)作为指示碳酸盐沉积氧化还原条件的重要指标:研究进展与问题评述[J].*古地理学报*,2018,20(4): 651-664.
- SHANG Mohan, TANG Dongjie, SHI Xiaoying, WEI Haoming, LIU Anqi. I/(Ca+Mg) as an important redox proxy for carbonate sedimentary environments: Progress and problems[J]. *Journal of Palaeogeography*, 2018, 20(4): 651-664.
- [25] 张俊鹏,李超,张元动.早古生代海洋缺氧事件的地质记录与背景机制[J].*科学通报*,2022,67(15): 1644-1659.

- ZHANG Junpeng, LI Chao, ZHANG Yuandong. Geological evidences and mechanisms for oceanic anoxic events during the Early Paleozoic[J]. *Chinese Science Bulletin*, 2022, 67(15): 1644-1659.
- [26] Kabanov P, Hauck T E, Gouwy S A, Grasby S E, Boon A v d. Oceanic anoxic events, marine photic-zone euxinia, and controversy of sea-level fluctuations during the Middle-Late Devonian[J]. *Earth-Science Reviews*, 2023, 241: 104415.
- [27] 李聪颖, 吴思璠. 大洋缺氧事件金属稳定同位素研究进展[J]. *地球科学进展*, 2022, 37(11): 1127-1140.
- LI Congying, WU Sifan. Advances in research on stable metal isotopes in Oceanic Anoxic Events[J]. *Advances in Earth Science*, 2022, 37(11): 1127-1140.
- [28] Dickson A J. A molybdenum-isotope perspective on Phanerozoic deoxygenation events[J]. *Nature Geoscience*, 2017, 10: 721-726.
- [29] Pearce C R, Cohen A S, Coe A L, Burton K W. Molybdenum isotope evidence for global ocean anoxia coupled with perturbations to the carbon cycle during the Early Jurassic[J]. *Geology*, 2008, 36(3): 231-234.
- [30] 王欢, 姚军明, 李杰. 钼同位素地球化学研究进展及其在成矿作用研究中的应用潜力[J]. *地球化学*, 2019, 48(3): 213-229.
- WANG Huan, YAO Junming, LI Jie. A review of progress in molybdenum isotope geochemistry and its potential application in mineralization research[J]. *Geochimica*, 2019, 48(3): 213-229.
- [31] Ostrander C M, Owens J D, Nielsen S G. Constraining the rate of oceanic deoxygenation leading up to a Cretaceous Oceanic Anoxic Event (OAE-2:~94 Ma)[J]. *Science Advances*, 2017, 3: e1701020.
- [32] Weyer S, Anbar A D, Gerdes A, Gordon G W, Algeo T J, Boyle E A. Natural fractionation of  $^{238}\text{U}/^{235}\text{U}$ [J]. *Geochimica et Cosmochimica Acta*, 2008, 72: 345-359.
- [33] 徐林刚.  $^{238}\text{U}/^{235}\text{U}$  分馏及其地质应用[J]. *矿床地质*, 2014, 33(3): 497-510.
- XU Lingang.  $^{238}\text{U}/^{235}\text{U}$  isotope fractionation in nature and its geological applications[J]. *Mineral Deposits*, 2014, 33(3): 497-510.
- [34] Dunk R M, Mills R A, Jenkins W J. A reevaluation of the oceanic uranium budget for the Holocene[J]. *Chemical Geology*, 2002, 190: 45-67.
- [35] Romanillo S J, Herrmann A D, Anbar A D. Uranium concentrations and  $^{238}\text{U}/^{235}\text{U}$  isotope ratios in modern carbonates from the Bahamas: Assessing a novel paleoredox proxy[J]. *Chemical Geology*, 2013, 362: 305-316.
- [36] Tissot F L H, Dauphas N. Uranium isotopic compositions of the crust and ocean: Age corrections, U budget and global extent of modern anoxia[J]. *Geochimica et Cosmochimica Acta*, 2015, 167: 113-143.
- [37] Lau K V, Maher K, Altiner D, et al. Marine anoxia and delayed Earth system recovery after the end-Permian extinction[J]. *Proceedings of the National Academy of Sciences of the United States of America*, 2016, 113: 2360-2365.
- [38] Zhang F F, Algeo T J, Romanillo S J, et al. Congruent Permian-Triassic  $\delta^{238}\text{U}$  records at Panthalassic and Tethyan sites: Confirmation of global-oceanic anoxia and validation of the U-isotope paleoredox proxy[J]. *Geology*, 2018, 46(4): 327-330.
- [39] Cheng K, Elrick M, Romanillo S J. Early Mississippian ocean anoxia triggered organic carbon burial and late Paleozoic cooling: Evidence from uranium isotopes recorded in marine limestone[J]. *Geology*, 2020, 48(4): 363-367.
- [40] Stirling C H, Andersen M B, Potter E K, Halliday A N. Low-temperature isotopic fractionation of uranium[J]. *Earth and Planetary Science Letters*, 2007, 264: 208-225.
- [41] Andersen M B, Romanillo S, Vance D, Little S H, Herdman R, Lyons T W. A modern framework for the interpretation of  $^{238}\text{U}/^{235}\text{U}$  in studies of ancient ocean redox[J]. *Earth and Planetary Science Letters*, 2014, 400: 184-194.
- [42] Chen X M, Romanillo S J, Herrmann A D, Wasylkeni L E, Anbar A D. Uranium isotope fractionation during coprecipitation with aragonite and calcite[J]. *Geochimica et Cosmochimica Acta*, 2016, 188: 189-207.
- [43] Chen X M, Romanillo S J, Hermann A D, Samankassou E, Anbar A D. Biological effects on uranium isotope fractionation ( $^{238}\text{U}/^{235}\text{U}$ ) in primary biogenic carbonates[J]. *Geochimica et Cosmochimica Acta*, 2018, 240: 1-10.
- [44] Tissot F L H, Chen C, Go B M, et al. Controls of eustasy and diagenesis on the  $^{238}\text{U}/^{235}\text{U}$  of carbonates and evolution of the seawater ( $^{234}\text{U}/^{238}\text{U}$ ) during the last 1.4 Myr[J]. *Geochimica et Cosmochimica Acta*, 2018, 242: 233-265.
- [45] Brennecke G A, Herrmann A D, Algeo T J, Anbar A D. Rapid expansion of oceanic anoxia immediately before the end Permian mass extinction[J]. *Proceedings of the National Academy of Sciences of the United States of America*, 2011, 108: 17631-17634.
- [46] Dahl T W, Boyle R A, Canfield D E, Connelly J N, Gill B C, Lenton T M, Bizzarro M. Uranium isotopes distinguish two geochemically distinct stages during the later Cambrian SPICE event[J]. *Earth and Planetary Science Letters*, 2014, 401: 313-326.
- [47] Dahl T W, Connelly J N, Kouchinsky A, Gill B C, Måansson S F, Bizzarro M. Reorganisation of Earth's biogeochemical cycles briefly oxygenated the oceans 520 Myr ago[J]. *Geochemical Perspective Letters*, 2017, 3(2): 210-220.
- [48] Elrick M, Polyak V, Algeo T J, et al. Global ocean redox variation during the middle late Permian through Early Triassic based on uranium isotope and Th/U trends of marine carbonates[J]. *Geology*, 2017, 45: 163-166.
- [49] Gilleadeau G J, Romanillo S J, Luo G M, et al. Uranium isotope evidence for limited euxinia in mid-Proterozoic oceans[J]. *Earth and Planetary Science letters*, 2019, 521: 150-157.
- [50] Zhang F, Lenton T M, Rey A, et al. Uranium isotopes in marine carbonates as a global ocean paleoredox proxy: A critical review[J]. *Geochimica et Cosmochimica Acta*, 2020, 287: 27-

- 49.
- [51] Andersen M B, Stirling C H, Weyer S. Uranium isotope fractionation[J]. *Reviews in Mineralogy & Geochemistry*, 2017, 82: 799-850.
- [52] Morford J L, Emerson S. The geochemistry of redox sensitive trace metals in sediments[J]. *Geochimica et Cosmochimica Acta*, 1999, 63: 1735-1750.
- [53] Andersen M B, Vance D, Morford J L, et al. Closing in on the marine  $^{238}\text{U}/^{235}\text{U}$  budget[J]. *Chemical Geology*, 2016, 420: 11-22.
- [54] Holmden C, Amini M, Francois R. Uranium isotope fractionation in Saanich Inlet: A modern analog study of a paleoredox tracer[J]. *Geochimica et Cosmochimica Acta*, 2015, 153: 202-215.
- [55] Rolison J M, Stirling C H, Middag R, et al. Uranium stable isotope fractionation in the Black Sea: Modern calibration of the  $^{238}\text{U}/^{235}\text{U}$  paleo-redox proxy[J]. *Geochimica et Cosmochimica Acta*, 2017, 203: 69-88.
- [56] Zhang F F, Xiao S H, Kendall B, et al. Extensive marine anoxia during the terminal Ediacaran Period[J]. *Science Advances*, 2018, 4: eaan8983.
- [57] Goto K T, Anbar A D, Gordon G W, et al. Uranium isotope systematics of ferromanganese crusts in the Pacific Ocean: Implications for the marine  $^{238}\text{U}/^{235}\text{U}$  isotope system[J]. *Geochimica et Cosmochimica Acta*, 2014, 146: 43-58.
- [58] Wang X L, Planavsky N J, Reinhard C T, Hein J R, Johnson T M. A Cenozoic Seawater redox record derived from  $^{238}\text{U}/^{235}\text{U}$  in ferromanganese crusts[J]. *American Journal of Science*, 2016, 316(1): 64-83.
- [59] Zhang F, Dahl T W, Lenton T M, et al. Extensive marine anoxia associated with the Late Devonian Hangenberg Crisis[J]. *Earth and Planetary Science Letters*, 2020, 533: 115976.
- [60] Helly J J, Levin L A. Global distribution of naturally occurring marine hypoxia on continental margins[J]. *Deep Sea Research Part I-Oceanographic Research Papers*, 2004, 51(9): 1159-1168.
- [61] Montoya-Pino C, Weyer S, Anbar A D, et al. Global enhancement of ocean anoxia during Oceanic Anoxic Event 2: A quantitative approach using U isotopes[J]. *Geology*, 2010, 38(4): 315-318.
- [62] Maher K, Steefel C I, DePaolo D J, et al. The mineral dissolution rate conundrum: Insights from reactive transport modeling of U isotopes and pore fluid chemistry in marine sediments[J]. *Geochimica et Cosmochimica Acta*, 2006, 70(2): 337-363.
- [63] Payne J L, Kump L. Evidence for recurrent Early Triassic massive volcanism from quantitative interpretation of carbon isotope fluctuations[J]. *Earth and Planetary Science Letters*, 2007, 256(1-2): 264-277.
- [64] Winguth C, Winguth A M E. Simulating Permian-Triassic oceanic anoxia distribution: Implications for species extinction and recovery[J]. *Geology*, 2012, 40(2): 127-130.
- [65] Burgess S D, Bowring S, Shen S Z. High-precision timeline for Earth's most severe extinction[J]. *Proceedings of the National Academy of Sciences*, 2014, 111(9): 3316-3321.
- [66] Stylo M, Neubert N, Wang Y, et al. Uranium isotopes fingerprint biotic reduction[J]. *Proceedings of the National Academy of Sciences of the United States of America*, 2015, 112(18): 5619-5624.
- [67] Noordmann J, Weyer S, Georg R B, et al.  $^{238}\text{U}/^{235}\text{U}$  isotope ratios of crustal material, rivers and products of hydrothermal alteration: New insights on the oceanic U isotope mass balance[J]. *Isotopes in Environmental and Health Studies*, 2015, 18: 1-23.
- [68] Reershemius T, Planavsky N J. What controls the duration and intensity of ocean anoxic events in the Paleozoic and the Mesozoic?[J]. *Earth-Science Review*, 2021, 221: 103787.
- [69] Tostevin R, Clarkson M O, Gangl S, et al. Uranium isotope evidence for an expansion of anoxia in terminal Ediacaran oceans[J]. *Earth and Planetary Science Letters*, 2019, 506: 104-112.
- [70] Wei G, Planavsky N J, Tarhan L G, et al. Marine redox fluctuation as a potential trigger for the Cambrian explosion[J]. *Geology*, 2018, 46: 587-590.
- [71] Wei G, Planavsky N J, He T, et al. Global marine redox evolution from the late Neoproterozoic to the early Paleozoic constrained by the integration of Mo and U isotope records[J]. *Earth-Science Reviews*, 2021, 214: 103506.
- [72] Dahl T W, Connelly J N, Kouchinsky A. Atmosphere-ocean oxygen and productivity dynamics during early animal radiations[J]. *Proceedings of the National Academy of Sciences of the United States of America*, 2019, 116(39): 19352-19361.
- [73] Bartlett R, Elrick M, Wheeley J R, et al. Abrupt global-ocean anoxia during the Late Ordovician-early Silurian detected using uranium isotopes of marine carbonates[J]. *Proceedings of the National Academy of Sciences of the United States of America*, 2018, 115: 5896-5901.
- [74] White D A, Elrick M, Romaniello S, et al. Global seawater redox trends during the Late Devonian mass extinction detected using U isotopes of marine limestones[J]. *Earth and Planetary Science Letters*, 2018, 503: 68-77.
- [75] Zhang F F, Shen S Z, Cui Y, et al. Two distinct episodes of marine anoxia during the Permian-Triassic crisis evidences by uranium isotopes in marine dolostones[J]. *Geochimica et Cosmochimica Acta*, 2020, 287: 165-179.
- [76] Jost A B, Bachan A, Schootbrugge B, et al. Uranium isotope evidence for an expansion of marine anoxia during the end-Triassic extinction[J]. *Geochemistry, Geophysics, Geosystems*, 2017, 18: 3093-3108.
- [77] Krause A J, Mills B J W, Zhang S, et al. Stepwise oxygenation of the Paleozoic atmosphere[J]. *Nature Communications*, 2018, 9: 4081.
- [78] Lenton T M, Daines S J, Mills B J W. COPSE reloaded: An improved model of biogeochemical cycling over Phanerozoic time[J]. *Earth-Science Reviews*, 2018, 178: 1-28.

- [79] Glasspool I J, Scott A C. Phanerozoic concentrations of atmospheric oxygen reconstructed from sedimentary charcoal[J]. *Nature Geoscience*, 2010, 3: 627-630.
- [80] Sperling E A, Wolock C J, Morgan A S, et al. Statistical analysis of iron geochemical data suggests limited late Proterozoic oxygenation[J]. *Nature*, 2015, 523 (7561): 451-454.
- [81] Belcher C M, McElwain J C. Limits for combustion in low O<sub>2</sub> redefine paleoatmospheric predictions for the Mesozoic[J]. *Science*, 2008, 321: 1197-1201.
- [82] Glasspool I J, Scott A C, Waltham D, et al. The impact of fire on the Late Paleozoic Earth system[J]. *Frontiers in Plant Science*, 2015, 6: 1-13.
- [83] Canfield D E. A new model for Proterozoic ocean chemistry[J]. *Nature*, 1998, 396: 450-453.
- [84] Canfield D E. In: Holland H D, Turekian, K K (Eds.). *Treatise on Geochemistry* [M]. New York: Elsevier, 2014: 197-216.

## Research advance for uranium isotope as a quantitative proxy for paleo-oceans anoxic or oxic environment

LUO Qukan<sup>1,2,3</sup>, CAO Jianhua<sup>2,3</sup>, ZHONG Liang<sup>2,3</sup>, BAI Bing<sup>2,3</sup>, WANG Qigang<sup>2,3,4</sup>, LIAO Hongwei<sup>2,3,5</sup>, ZONG Keqing<sup>1</sup>, QIN Hanlian<sup>2,3</sup>

(1. School of Earth Sciences, China University of Geosciences, Wuhan, Hubei 430078, China; 2. Institute of Karst Geology, CAGS/Key Laboratory of Karst Dynamics, MNR & GZAR/International Research Center on Karst under the Auspices of UNESCO, Guilin, Guangxi 541004, China; 3. Pingguo Guangxi, Karst Ecosystem, National Observation and Research Station, Pingguo, Guangxi 531406, China; 4. School of Environmental Studies, China University of Geosciences, Wuhan, Hubei 430078, China; 5. Key Laboratory of Geological Survey and Evaluation of Ministry of Education, China University of Geosciences, Wuhan, Hubei 430078, China)

**Abstract** Compared with other elements that are sensitive to redox environments (U, Mo, V, S, Fe, Cu, Zn, Ni), uranium isotopes have the advantage to quantitatively reflect long-term and global-scale paleoredox of oceans, due to its uniform composition in the oceans globally, and quantitative relationship with the proportion of the anoxic seafloor areas in ancient oceans. Therefore, uranium isotopes are widely used in the events such as the Late Ediacaran, Early Cambrian, Ordovician/Silurian, Late Devonian, Devonian/Carboniferous, Permian/Triassic, Triassic/Jurassic, and OAE 2 (Oceanic Anoxic Event 2). Through a review of previous papers, the author has systematically summarized the principles, methods, and results of using uranium isotopes for quantitative analysis of paleoredox. It has found that the core of current uranium isotopes quantitative method is the mass balance box model of seawater uranium (mass balance box model) and its isotopes and the related variants. By simplifying the uranium mass balance box model based on the proportion and fractionation coefficient of different types of uranium sinks, the redox environment and duration of ancient oceans can be quantitatively reflected. However, there may be ambiguity in the interpretation regarding whether the marine environment contains sulfur or not.

In addition, by reviewing previous papers, the author has set up a preliminary coupling relationship among the proportion of anoxic seafloor area (%) reflected from uranium isotopes, atmospheric oxygen concentration, and oceanic anoxic or biological events. It has found that: (1) the uranium isotope analysis results were highly consistent with the occurrence time and extent of various anoxic or biological events, especially being coincident with the events that occurred in the Late Ediacaran, Late Ordovician, Late Devonian Frasnian-Famennian, Devonian/Carboniferous, Permian/Triassic, and Triassic/Jurassic periods, indicating that uranium isotopes are indeed an effective global scale and deep-time scale proxy for quantitative analysis on paleoredox of oceans. (2) The trend of anoxic seafloor expansion is not completely consistent with the trend of the atmospheric oxygen concentration changes. Usually, there is a lag. Only the trend of atmospheric oxygen concentration changes in the Triassic/Jurassic period is similar to the trend of oceanic redox environment changes. Analysis suggests that uranium isotope analysis results indicate the proportion of anoxic seafloor area, that is, the proportion of anoxic bottom seawater area, which is actually the change of redox environment of oceanic bottom water. At first, the change in atmospheric oxygen concentration affects shallow seawater, which first responds to the changes in the atmospheric redox environment, and then gradually affects the biological productivity of the seawater, gradually transmitting the environmental changes caused by redox

evolution to the bottom water, and thus leading to a lag reaction of anoxic seafloor's expansion or shrink; or due to climatic changes, sea level rise and fall can cause changes of ocean internal circulation (such as thermohaline ocean circulation), leading to changes in productivity and causing anoxic seafloor area expansion or shrink, which may also result in hysteresis effects. There should be a kind of coupling relationship between the atmospheric redox evolution and ocean redox evolution, it deserves to be paid more attention for further study in future.

In addition, through a review and analysis of previous research results, the author believes that there are several problems with the quantitative analysis of global scale paleoredox environments of oceans by using uranium isotopes, such as low accuracy, ambiguity, and the representativeness of samples. It is suggested to improve this method from the following two aspects further: (1) although uranium isotopes have been widely used in many important biological events or oceanic anoxic events since the Ediacaran period, the representativeness of sampling sites for some research results still needs to be improved. Although uranium isotopes are assumed to have global homogeneity theoretically, this assertion has not fully considered the influence of post-diagenesis, weathering and alteration in each sampling site on the uranium isotope composition that reflects the original seawater features. It is necessary to calibrate and verify the analysis results of different samples from different sampling sites of the same period to improve the quantitative analysis accuracy further. (2) The single proxy analysis results of uranium isotopes provides a wide range of anoxic seafloor area proportion, showing insufficient accuracy. It is necessary to carry out comprehensive multi-proxy isotopic quantitative analysis, by adding the results of isotopes like Mo, Tl, and others, which is believed could effectively improve the analysis accuracy for the same event.

Finally, the author believes that if the accuracy of uranium isotopes method for quantitative analysis could be improved by comprehensive analysis with combination of other isotopes analysis, it is necessary to find out the coupling relationship between atmospheric redox evolution and marine redox evolution, especially the time effects of marine redox evolution to the atmospheric evolution. Hence, it is also possible to find out the response mechanism of oceanic redox conditions to the atmospheric redox evolution. The coupling relationship and the response mechanism may help the related researchers to predict the impact range and extent of oceanic redox evolution after a certain periods of lagging to the atmospheric redox evolution that is caused by natural and human factors. The results may provide great support for addressing global climate change.

**Key words** uranium isotope, quantitative reflection, uranium isotope model, oceanic anoxic events, biological events

( 编辑 张玲 )